A potential climatic index for total Saharan dust: the Sun insolation

P. Alpert, J. Barkan, and P. Kishcha

Department of Geophysics and Planetary Sciences, Tel-Aviv University, Tel-Aviv, Israel

Received 21 April 2005; revised 10 July 2005; accepted 21 October 2005; published 11 January 2006.

[1] It is shown that the daily course of the total amount of dust in the atmosphere, based on the TOMS aerosol index (AI), is highly correlated (0.98) with the integrated daily solar insolation over the Sahara region for spatially and temporally averaged data. Moreover, the annual maximum is even reached nearly at the same day, i.e., the 17th (18th) June for the surface (top of the atmosphere) solar insolation, as compared to 21st June for the date of maximum atmospheric dust loading. Other factors like cloudiness, rainfall soil moisture, and wind probably play a more dominant role in smaller areas. The fact that on a very large scale, like the whole of the Sahara, the solar insolation becomes the one single forcing directly correlated with the total amount of dust in the atmosphere is suggesting a simple climatic index for the total dust loading in the atmosphere. This index is shown for the Saharan region only, while more studies are needed for other regions. The 3–4 day time-lag between the maximum insolation and the maximum dust loading in the atmosphere is compared to about a one-month delay with the maximum ground or air temperatures and may serve as an estimate to the surface response to the major forcing of the Sun. The maximum ground temperature, delayed to the 17th July, can be explained by the delay in the lagged-heating of the deeper soil layers. The 3–4 day delay only with the Sun insolation is probably linked to the period in which the dust is maintained in the atmosphere until it is deposited. One application to the present finding may be for climate models, since such a high correlation for spatially and temporarily averaged data may be used as an integrated index for the total amount of Saharan dust and for potentially validating the complex model parameterizations in climate models.

Citation: Alpert, P., J. Barkan, and P. Kishcha (2006), A potential climatic index for total Saharan dust: the Sun insolation, *J. Geophys. Res.*, *111*, D01103, doi:10.1029/2005JD006105.

1. Introduction

[2] The local generation of mineral dust is directly related to the uplifting dust processes that were studied quite extensively [e.g., *Bagnold*, 1965; *Balkanski et al.*, 1996]. It was found that wind intensity, amount of vegetation, soil moisture and atmospheric stability are some of the key variables. For instance, *Nickovich et al.* [2001] adopted the following formula for the dust concentration (later also used by *Alpert et al.* [2002]).

[3] Surface concentration [*Shao et al.*, 1993]:

$$C_s = \text{const} * \delta_k u_*^2 \left[1 - \left(\frac{u_{*t}}{u_*}\right)^2\right], \quad \text{for} \quad u_* \geq u_{*t} \qquad (1)$$

where C_s is the surface concentration, δ_k is the dust productivity factor (depending on vegetation, soil texture and available soil mass for uplift), u_* is the friction velocity and u_{*t} is the threshold friction velocity.

[4] While the surface fluxes viscous sublayer [*Jancic*, 1994] is

$$C_0 = \frac{C_s + \omega C_{LM}}{1 + \omega}, \qquad \omega = \frac{\left(\frac{K_{Csfc}}{\Delta z}\right)}{\left(\frac{\lambda}{Z_c}\right)}, \qquad (2)$$

where C_0 is the concentration at the interface of the viscous and turbulent layer, C_{LM} is the concentration of the lowest model level, ω is the ground wetness predicted by the atmospheric model, K_{Csfc} is the surface mixing coefficient, Δz is the depth of the lowest model layer, λ is the viscous diffusivity for dust concentration and z_C is the height of the viscous sublayer (which is linked to the surface temperature).

[5] The threshold friction velocity u_{*t} is directly related to the soil moisture with the following formula [*Fecan et al.*, 2000]:

$$\begin{aligned} u_t &= U_{*t}, && \text{for } w \leq w' \text{ (dry soil)} \\ u_{*t} &= U_{*t}\sqrt{1 + 1.2(w - w')^{0.68}}, && \text{for } w > w' \text{ (wet soil)} \end{aligned} \qquad (3)$$

where U_{*t} is threshold minimum friction velocity and w' is the maximum amount of adsorbed water in the soil. These

0148-0227/06/2005JD006105$09.00

set of equations demonstrate an example of how soil moisture, surface wind and surface temperature are affecting the dust generation [*Nickovich et al.*, 2001].

[6] In the aforementioned formulations, the solar insolation, i.e. the downwelling solar flux averaged over the day, is not explicitly incorporated. However, as shown next, the solar heating is implicitly responsible for the major processes of both dust uplifting and of the maintaining of the high amounts of dust in the atmosphere. Solar daily heating of the land surface is the major forcing for buoyant production of turbulent kinetic energy (TKE) on days of free convection [*Stull*, 1988].

[7] The second important term in generation of TKE is the mechanical shear production, which is proportional to the square of the vertical wind shear, $(\partial\overline{u}/\partial z)^2$, near the surface. Over the Sahara region, with generally clear skies and hot surface the major contributor to turbulence seems clearly to be the buoyant production, which is proportional to the surface heat fluxes. On the one hand, the mechanical (shear) production may be playing the primary role in the local uplifting and is also intensified with strong solar insolation [*Alpert and Eppel*, 1985]. On the other hand, however, strong buoyancy on such days is also responsible for keeping the dust up in the turbulent atmospheric boundary layer and delaying any significant deposition. Hence, both terms, directly linked to the solar insolation explain why the insolation may be a better index (compared to the other potentially correlated variables), for the total integrated amount of dust in the atmosphere on a daily basis.

[8] The purpose of the present note is to explore the direct relationship between the total amount of the dust over a large region and the amount of solar insolation. It will be shown by employing the Total Ozone Measuring Spectrometer – Aerosol Index (TOMS-AI [*Herman and Celarier*, 1997]), that indeed the total column amount of dust averaged over the whole Sahara region is highly correlated with the integrated daily solar radiation at the surface, i.e. the solar insolation over climatic periods. Moreover, the maximum solar insolation is followed by the maximum dust loading with a lag of a few days. This is the shortest time lag as compared to those for the time lags of other relevant variables like, wind, ground temperature, air temperature and soil moisture.

[9] Next, section 2 describes the methodology and data processing. Section 3 presents the results and is followed by the discussion (section 4) in which the significance of these results will be highlighted.

2. Methodology and Data Processing

[10] The linkage between the solar radiation and the integrated dust amount in the atmosphere over the Sahara desert, were determined. For this, the daily data of the TOMS-Aerosol Index and the solar radiation at the top of the atmosphere (TOA) as well as the solar insolation, were used. Additionally, in order to estimate the influence of the ground moisture and the ground or air temperature on this linkage, daily data of these variables from the NCEP/NCAR reanalysis, were employed. The correlation between TOA radiation from the reanalysis and TOA theoretical value was found to be very high, 0.99.

[11] The Total Ozone Mapping Spectrometer Aerosol Index (AI) daily data were used to estimate an index for the total dust amount over a given area with a spatial resolution of 1.25° longitude and 1° latitude [*Herman and Celarier*, 1997]. This index utilizes the spectral contrast of two ultraviolet channels: 340 nm and 380 nm. It is positive for dust and provides an index for the integrated amount of the aerosol in the column along the line of sight. The TOMS-AI index is an effective measure for dust mainly at altitudes higher than 1 km, and was also shown to be effective in improving the dust initialization in dust prediction models [*Alpert et al.*, 2002]. Concerning the reliability of the AI calculation below 1 km, *Herman and Celarier* [1997] indicated that UV-absorbing aerosols in the boundary layer near the ground could not readily be detected by this method. It means that the accuracy of AI is low below 1 km. However, *Torres et al.* [2002] consider that for mineral dust this restriction for TOMS AI is not so important and that AI allows the detection of dust particles even close to the ground. The clear advantage of the TOMS-AI, however, is, that due to the very low albedo of the UV particularly above land, it is able to provide a dust measure everywhere above land and sea [*Prospero et al.*, 2002]. An advantage of the TOMS is that it is a dust-measuring instrument which has been operating since 1979. Missing TOMS-AI values were not incorporated in the averaging; fortunately, cloudy regions are very limited over the Sahara [e.g., *Shay-El et al.*, 1999]. Number of missing values over the Sahara for a specific point, were found to be about 1% (for instance, 3–4 missing points out of 434 for 14 months of June).

[12] For the TOA radiation, the surface radiation, the ground moisture and the temperature data, the NCEP/NCAR reanalysis, was employed [*Kalnay et al.*, 1996]. The unit of the radiation data is W/m^2. The moisture and the ground temperature are measured at 0–10 cm below the ground level and the air temperature at 2 m above ground. The unit of the moisture is m^3/m^3 and of the temperature is in degrees Celsius. For all these parameters daily averages as provided by NCEP/NCAR reanalysis, were employed. These averages are based on 6-h interval values and the spatial resolution corresponds to a horizontal interval of $2.5° \times 2.5°$.

[13] The period of this work includes 14 years from the 1 Jan 1979 to 31 Dec. 1992. For every variable, the average of the 14 data points for every day was computed. The correlations between the daily AI and the average TOA and surface radiation as well as with the ground or air temperatures, were computed. The multiple regression between the AI as the dependent variable and the radiation and ground moisture, were also calculated.

[14] The full study area of 20°N–35°N and 15°W–60°E includes the Saharan desert and the Arabian Peninsula. This is a large area and local effects are largely smoothed out. In addition, results for three subareas for the same dust-laden latitudinal zone i.e., 20°N–35°N, were also derived, as follows: West Sahara for 15°W–10°E, East Sahara for 10°E–40°E and Saudi-Arabia for 40°E–60°E (Figure 1). The semi-desert region south of the Sahara (the Sahel), with the southern border at 15°N was also incorporated in additional experiments but with very similar results (not shown).

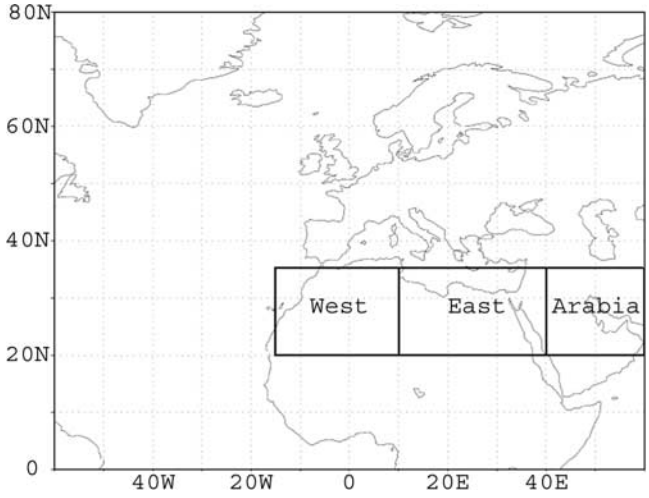

Figure 1. Map of the data acquisition area and the subareas.

[15] For the whole area as well as subareas, the plots prepared show the 14 year averages as function of the day throughout the year. Separate graphs of the AI and temperature against the TOA and the surface radiation, were plotted. Since, however, the TOA and surface radiation correlation values (with TOMS-AI) were found almost identical, only the surface radiation results, are presented. Additional graphs were prepared of AI against ground moisture and temperature. For the temperature and the moisture only the cases for the whole area are shown. The results for radiations, moisture and temperature are summarized in Tables 1 and 2.

3. Results

3.1. Dust and Radiation

[16] Figure 2 shows the annual daily courses of the integrated insolation and dust loading. The two curves reach their peak almost simultaneously at 17th and 21st June, respectively. *Barkan et al.* [2004] have already shown, but for monthly averages, that the annual peak of the TOMS-AI occurs in June for the whole Sahara region. The peak date in Figure 2 is obvious for the radiation that follows the Sun but it is quite remarkable for the dust in spite of the large variability and many factors that are supposed to influence its amount in the atmosphere, e.g., equations (1)–(3). The ascent of the dust amount from the winter months through the spring toward June is somewhat slower that its descent through the fall months indicating less dust activity in the early spring and rapid rise of the activity especially in May. The correlation between the average radiation and the average dust daily courses throughout the year is 0.97–0.98 (Table 2). The correlation between AI and the theoretical value of TOA solar radiation [*Liou*, 1980], was also calculated and found to be 0.975.

[17] The maximum dust is reached on June 21, the TOA radiation on June 18 and the surface radiation on June 17 (Table 1). It should be noted that for individual years the correlation drops to an average value of 0.91 ± 0.02. This is not unexpected since inter-annual dust variability can be high [e.g., *Barkan et al.*, 2004] due to climate factors like, for instance, the North Atlantic oscillation (NAO [i.e., *Moulin et al.*, 1997]).

[18] The annual course of the dust relative to the radiation is quite different in the western subregion of the Sahara (Figure 3a). The ascent of the dust amount is quite low in the spring months (relative to the radiation curve) but increases steeply during June–July. Accordingly, the peak AI at the West Sahara occurs only at July 9–10 almost one month after the radiation maximum (Table 1). The correlation is 0.89–0.9 and is lower due to the deviation of the dust from the radiation in spring and summer, (Table 2). This deviation is also related to the major activity of the main dust sources in the western region, i.e., in Mali, Mauritania and the Spanish Sahara, in the summer months [*Prospero et al.*, 2002; *Washington et al.*, 2000; *Barkan et al.*, 2004].

[19] The annual course of the dust in the eastern subregion is almost in the opposite sense to that of the west. The ascent of the dust amount during the early spring months is rapid, approximately paralleling the radiation curve. Consequently, the peak dust value is reached already in the second half of May, then descents rapidly, much steeper compared to the radiation curve. There are also two secondary peaks, one in the beginning of July and one in September (Figure 3b). Accordingly, the AI peak is in May 17, one month earlier than the radiation peak (Table 1). The correlation here is again lower, i.e., 0.91–0.92 as compared to that for the whole area (Table 2). The main cause of this dust pattern is assumed to be the prominent dust source of the Bodele depression (18°N, 19°E) whose peak activity occurs in May [*Prospero et al.*, 2002; *Washington et al.*, 2000; *Barkan et al.*, 2004]. Another contributor is the fact that April and May are the peak time for the Sharav cyclones along the eastern Mediterranean coast of Africa. These shallow, warm and extremely active disturbances lift huge amounts of dust in the eastern subregion. Lower intensity Sharav cyclones mainly in September may be associated with the secondary dust peak in this month [*Alpert and Ziv*, 1989; *Dayan et al.*, 1991].

Table 1. Maximum Values of Top of the Atmosphere Radiation, Surface Radiation, Aerosol Index and 0–10 cm Below Ground Temperature in Different Regions of the Sahara (Whole Area, West Sahara, East Sahara, and Saudi Arabia; See Figure 1) and the Date of Their Occurrence[a]

Variables → Maximum Values Region ↓	Maximum Aerosol Index Date in Parenthesis	Maximum Surface Radiation, W/m^2 Date in Parenthesis	Maximum TOA Radiation, W/m^2 Date in Parenthesis	Maximum Temperature 0–10 cm Below Ground, °C Date in Parenthesis
Whole Area	1.76 (21 Jun)	377.07 (17 Jun)	472.14 (18 Jun)	32.18 (17 Jul)
West Sahara	2.23 (10 Jul)	364.29 (16 Jun)	472.14 (18 Jun)	32.5 (9 Jul)
East Sahara	1.62 (17 May)	380.37 (14 Jun)	472.14 (18 Jun)	30.84 (18 Jul)
Saudi Arabia	1.77 (24 Jun)	391.87 (21 Jun)	472.14 (18 Jun)	33.82 (25 Jul)

[a]Calculations were based on average values 1979–1992.

Table 2. Correlation Coefficients for the Four Different Regions of the Sahara (as in Table 1) Based on 1979–1992 TOMS-AI and NCEP/NCAR Reanalysis Data

Correlation Coefficients → Region ↓	AI Versus TOA Radiation[a]	AI Versus Surface Radiation[b]	AI Versus TOA Radiation and Moisture[c]	AI Versus Surface Radiation and Moisture[d]	TOA Radiation Versus Ground Temperature,[e] T_g	Surface Radiation Versus Ground Temperature,[f] T_g
Whole Area	0.97	0.98 (Figure 2)	0.97	0.98	0.91[g]	0.93
West Sahara	0.9	0.89 (Figure 3a)	0.9	0.91	0.9	0.89
East Sahara	0.92	0.9 (Figure 3b)	0.96	0.95	0.91	0.92
Saudi Arabia	0.96	0.97 (Figure 3c)	0.96	0.97	0.92	0.96

[a]AI versus TOA radiation.
[b]AI versus surface radiation.
[c]AI versus TOA radiation and soil moisture (multiple regression).
[d]AI versus surface radiation and soil moisture (multiple regression).
[e]TOA radiation versus 0–10 cm below ground temperature.
[f]Surface radiation versus 0–10 cm below ground temperature.
[g]AI versus T_g yields 0.90, while AI versus T_a yields 0.87.

[20] The 14-y average dust course over the Arabian Peninsula is quite similar to that of the whole area (Figure 3c). The AI curve follows closely the radiation curve and the peak values are June 21 and June 24 respectively (Table 1) with a correlation value of 0.96–0.97 (Table 2).

[21] The fact that the dust follows the radiation so closely over the whole region seems the result of the balance between the opposite deviations of the dust in the western and eastern subregions. However, the case of the Arabian Peninsula indicates that when smoothing-out the synoptic and all local topographical influences, the radiation and the dust values tend to change simultaneously throughout the year.

3.2. Dust and Ground Factors: Ground Moisture and Surface Temperature

[22] Next, the ground moisture and the surface ground/air temperature linkages with the dust, were examined, assuming that both factors influence the dust uplifting into the atmosphere (section 1). According to the theory, i.e., equations (1)–(3), the ground moisture hinders the lifting of the dust, while high temperatures strengthen convection and enhance it.

[23] Figure 4 shows the average daily AI value along the year along with the average ground moisture for the whole area. The subareas show similar results (not shown). One can see that the maximum soil moisture occurs in late winter and early spring months compared to the dust peak in June. Accordingly, the correlation is only −0.3. To assess the influence of moisture on the correlation between the radiation and the AI, the multiple regression of the AI against both the radiation and the moisture for the whole area as well as for the subareas separately, were computed (Table 2). No significant improvement was achieved compared to the correlation with radiation only.

[24] Figure 5 shows the average daily ground radiation along with the averaged ground temperature (T_g). As

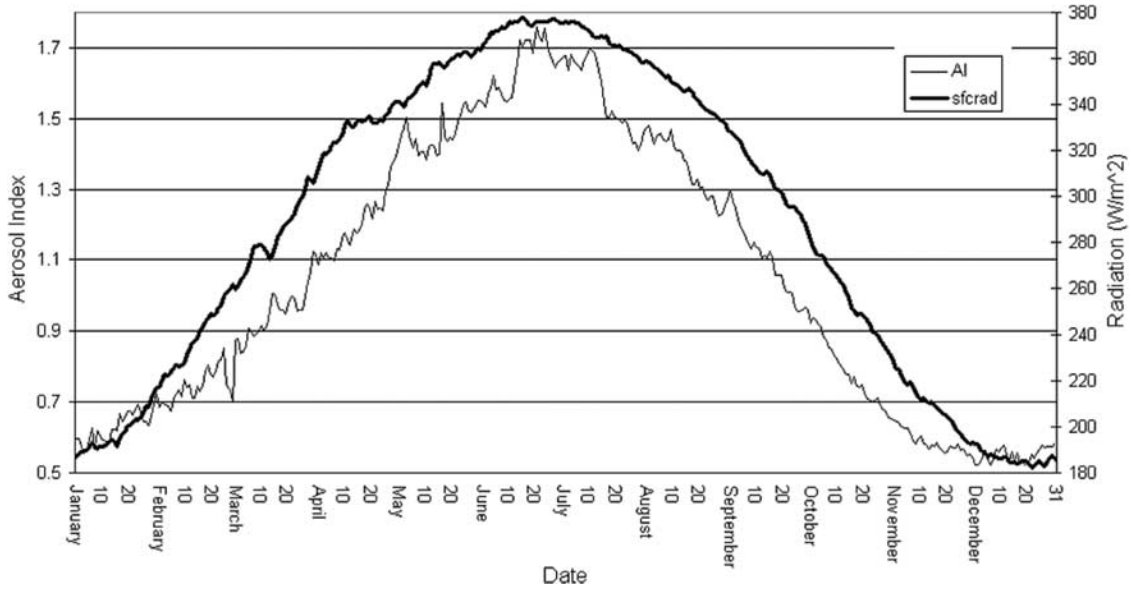

Figure 2. Mean annual variations of the aerosol index and the surface radiation, 1979–1992 averaged over the whole area: 15W–60E, 20N–35N. Correlation coefficient is 0.98.

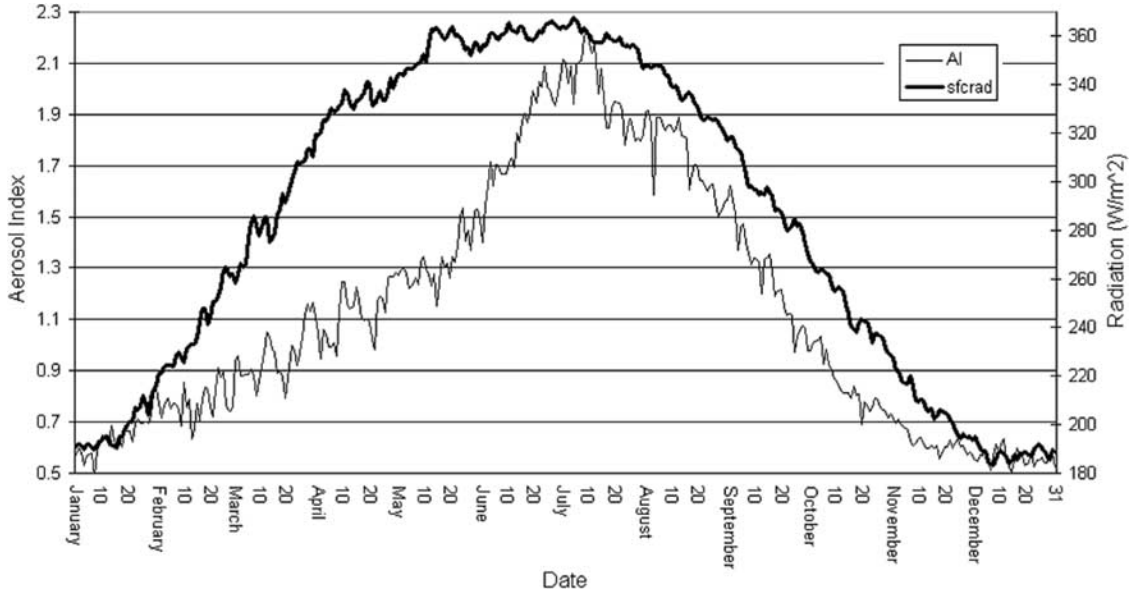

Figure 3a. Mean annual variations of the aerosol index and the surface radiation, 1979–1992 averaged over the West Sahara region, i.e., 15W–10E, 20N–35N. Correlation coefficient is 0.89.

expected, there is a good agreement between the course of the surface radiation and that of the ground temperature with a correlation coefficient of 0.91 (Table 2). Note that there is a delay of approximately one month of the peak value of the ground temperature relative to the surface radiation (and hence to the dust), i.e., 17 July (for T_g) compared to 17th June (for radiation) and 21 June (for AI) (Table 1). The correlation between TOMS-AI and the air temperatures, T_a, was also calculated; minor changes were found as follows. The peak air temperature T_a, lags the dust peak by 28 d while the ground temperature, T_g, lags by 23 d. In both cases, the maximum lagged-correlations (of 28 d or 23 d) reach about 0.98. The reason T_g has a shorter lag may be due to the additional factor of soil moisture strongly linked to the T_g rather than T_a. Note that in Table 2 the maximum lagged-correlation with the ground temperature is 26 d (not 23 d) because the 23 d calculation was based on running averages.

4. Discussion and Conclusions

[25] It seems that there is no other external variable which shows such a high unlagged correlation (0.98) with the total amount of dust in the atmosphere like the integrated daily

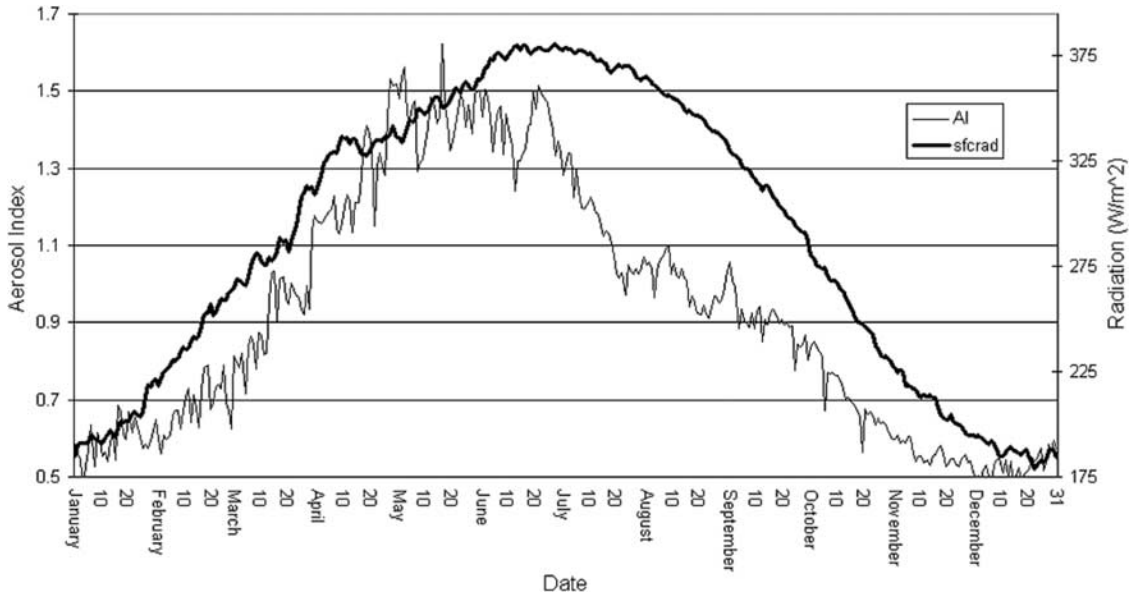

Figure 3b. Same as in Figure 3a, but for the East Sahara region, i.e., 10E–40E, 20N–35N. Correlation coefficient is 0.9.

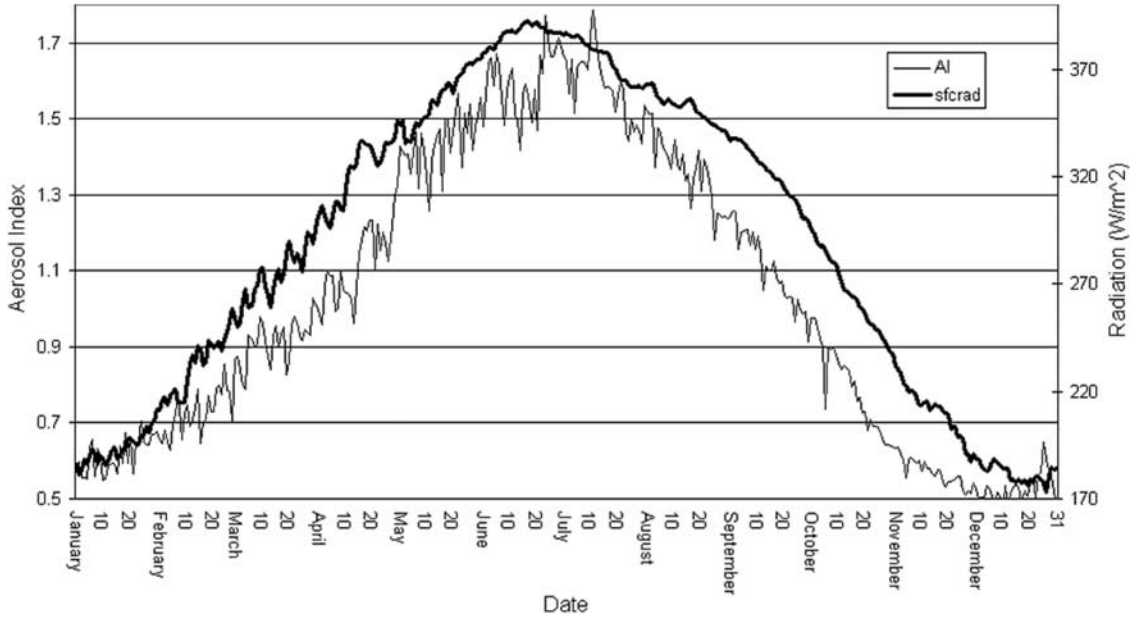

Figure 3c. Same as in Figure 3a, but for the Saudi-Arabia region, i.e., 40E–60E, 20N–35N. Correlation coefficient is 0.97.

solar insolation as shown here, for the first time. Moreover, the annual maxima are even reached at very close dates, i.e., the 17th (18th) June for the surface (top of the atmosphere) solar insolation, as compared to 21st June for the date of maximum atmospheric dust loading based on the TOMS-AI. (The sensitivity of the TOMS-AI to the dust altitude as discussed in section 1 seems to be less critical over the Sahara where the boundary-layer height could easily reach 3–5 km around noontime when the TOMS-AI is relevant. *Charney* [1975], for instance, assumed BL height of about 5 km over the Sahara.) As expected, the high correlation drops when smaller subregions are considered. For instance, in the East (or West) Sahara only, the correlation value with surface insolation drops from 0.98 to 0.9 (0.89). With even further shrinking of the inspected region to $4^\circ \times 4^\circ$ subregion squares only (not shown), the correlation values drop further to about 0.74–0.88. This is not surprising since in smaller regions the synoptics as well as the local terrain become increasingly dominant factors in the dust up lifting. These factors include, for instance, the following local mechanisms like topographical effects, lee cyclogenesis, inter-tropical convergence zone and the preferred areas of dust sources [*Barkan et al.*, 2004; *Prospero et al.*, 2002]. Other factors like cloudiness, rainfall and soil moisture also play an increasingly dominant role in smaller areas. Similarly, the correlation drops for a specific season (not full

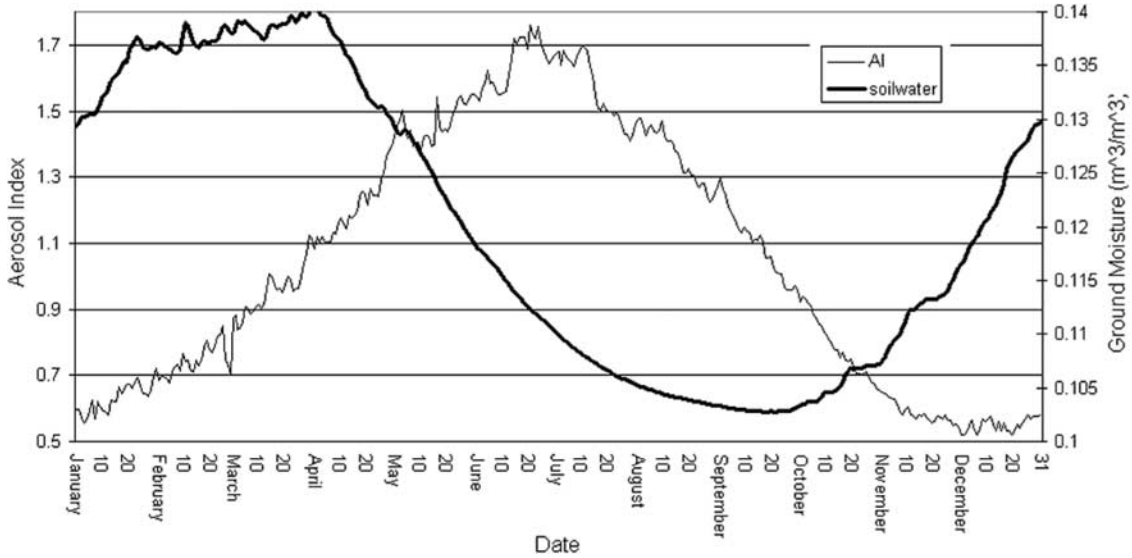

Figure 4. Mean annual variations of the aerosol index and the ground moisture (0–10 cm), 1979–1992 averaged over the whole area 15W–60E, 20N–35N. Correlation coefficient is −0.3.

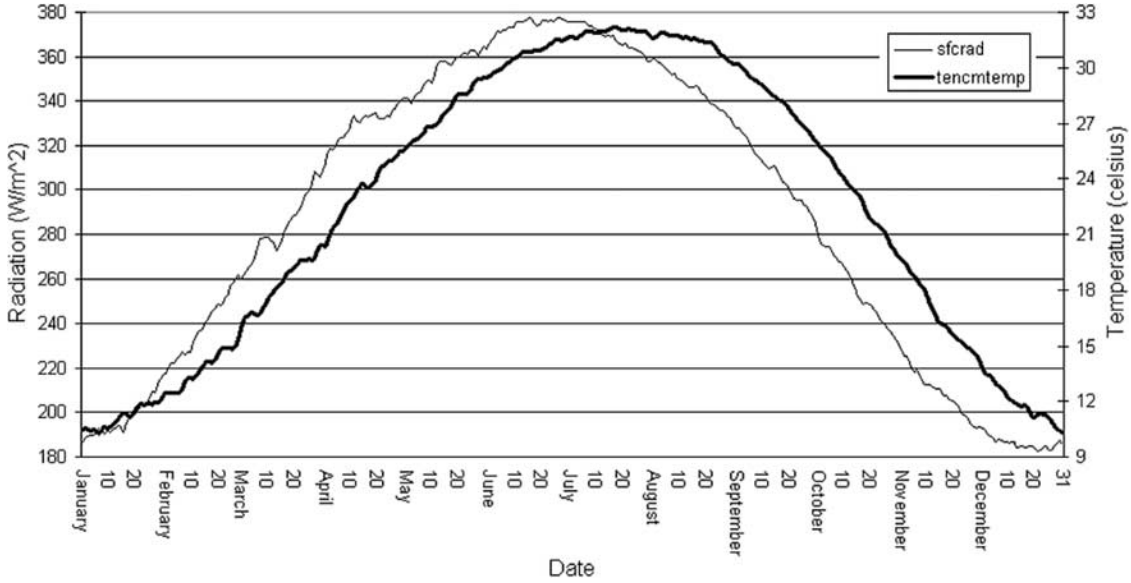

Figure 5. Mean annual variations of the surface radiation and the ground temperature (0–10 cm; surface temperature in the plot) 1979–1992 averaged over the whole area 15W–60E, 20N–35N. Correlation coefficient is 0.93.

year) to as low as 0.5 in winter (DJF) and 0.88 for autumn (SON). Hence, for climate model's typical grid size of several degrees, it seems that the dust indexing for the whole Sahara region may be quite useful mainly for climatic periods of about one decade and larger. The fact that on a very large scale like the whole of the Sahara, the solar insolation becomes the one single forcing directly correlated (0.98) with the total amount of dust in the atmosphere on a given day is from a first thought quite surprising. With a second thought this may be explained, since both the dust uplifting mechanisms, i.e. strong near-surface wind shears, as well as the dust maintaining mechanism in the atmosphere, i.e., strong buoyancy, are often directly related, to the surface solar insolation. Furthermore, the dryness of the top layer of the Earth's ground (0–2 cm) is also directly related to the solar insolation with a relatively short time-delay of about one day.

[26] Another puzzling question is that the dust radiative impacts have probably not been considered in the reanalysis in computing the solar radiation. Hence, the extinction within the dust layer would result in less solar radiation at the surface. Thus, more dust loading will result in less downward solar radiation and will lead to a negative feedback, compared to analysis in this study, which may result in the decrease of correlation. The answer to this may lie in the fact that the heating induced by the solar radiation absorbed in the dust layer [*Alpert et al.*, 1998; *Kishcha et al.*, 2003], is also another contributor to maintaining of the dust in the atmosphere by increasing the thermal energy and the potential buoyancy of the absorbing dust layer. It could well be that this positive feedback compensates for the negative feedback.

[27] It is very interesting that the ground temperature lags by about one month after the maximum amount of dust (17th July versus 21st June, Table 1). Hence, it is not the ground temperature (0–10 cm, Table 2) that reaches the maximum correlation (0.93) with dust, but the solar insolation. As already discussed earlier, the air temperature correlation with dust is similar, i.e., AI&Tg → 0.90 compared AI&Ta → 0.87.

[28] The 3–4 day time lag between the maximum insolation and the maximum dust loading in the atmosphere is of interest for the understanding of atmospheric and surface response to the major solar forcing. The maximum ground temperature, delayed by about one month, from 17th June to 17th July may not be too surprising since the delay in the nearby oceans heat capacity as well as the delay in the heating of the deeper soil layers contribute much to the atmospheric delay [e.g., *Geiger*, 1965].

[29] The 3–4 day delay in the integrated dust loading compared to the Sun's insolation forcing, may be at least partly explained by the period in which the dust stays in the atmosphere prior to its deposition. If indeed this is the main contribution to the delay, then we may assume that the 3–4 day delay provides an indirect measure for the average period of the dust residence time in the atmosphere. This 3–4 day period is most reasonable for the total dust loading, since the coarse dust particles are deposited within 1–2 days, while the fine particles can stay in the atmosphere over a week [*Prospero et al.*, 2002; *Kaufman et al.*, 2005]. It should be noted however, that this delay between the maximum insolation and the maximum dust (AI) varies for individual years during 1979–1992 between −5 to +5 d (reaching even ±8 days in two of the years) due to the large inter-annual variability in the dust and the climate factors. Hence, the long term 14-y average lag result is obviously of relevance primarily for long climate runs, not for individual years.

[30] One potential application to the present finding may be the direct incorporation of the solar insolation in dust prediction climate models. This may be particularly useful for climate models, since such a high correlation of 0.98,

i.e., between surface insolation and integrated dust, may be used as an integrated index for the evaluation of the model parameterizations for dust in long climatic runs.

References

Alpert, P., and A. Eppel (1985), A proposed index for mesoscale activity, *J. Clim. Appl. Meteorol.*, *24*, 472–480.

Alpert, P., and B. Ziv (1989), The sharav cyclone: Observations and some theoretical considerations, *J. Geophys. Res.*, *94*(D15), 18,495–18,514.

Alpert, P., Y. Shay-El, Y. J. Kaufman, D. Tanre, A. da Silva, S. Schubert, and J. H. Joseph (1998), Quantification of dust-forced heating of the lower troposphere, *Nature*, *395*(6700), 367–370.

Alpert, P., S. O. Krichak, M. Tsidulko, H. Shafir, and J. H. Joseph (2002), A dust prediction system with TOMS initialization, *Mon. Weather Rev.*, *130*(9), 2335–2345.

Bagnold, R. A. (1965), *The Physics of Blown Sand and Desert Dunes*, 265 pp., Methuen, New York.

Balkanski, Y., M. Schulz, B. Marticorena, G. Bergametti, W. Guelle, F. Dulac, C. Moulin, and C. E. Lambert (1996), Importance of the source term and the size distribution to model the mineral dust cycle, in *The Impact of Desert Dust Across the Mediterranean*, edited by S. Gurzoni and R. Chester, pp. 69–76, Springer, New York.

Barkan, J., H. Kutiel, and P. Alpert (2004), Climatology of dust sources in North Africa and the Arabian Peninsula, based on TOMS data, *Indoor Built Environ.*, *13*(407–419), doi:10.1177/1420326x04046935.

Charney, J. G. (1975), Dynamics of the desert drought in the Sahel, *Q. J. R. Meteorol. Soc.*, *101*, 193–202.

Dayan, U., J. Hefter, J. Miller, and G. Gutman (1991), Dust intrusion events into the Mediterranean Basin, *J. Appl. Meteorol.*, *30*, 1185–1199.

Fecan, F., B. Marticorena, and G. Bergametti (2000), Parameterization of the increase of the Aeloian erosion threshold wind friction velocity due to soil moisture for arid and semi-arid areas, *Ann. Geophys.*, *17*, 144–157.

Geiger, R. (1965), *The Climate Near the Ground*, 611 pp., Harvard Univ. Press, Cambridge, Mass.

Herman, J. R., and E. Celarier (1997), Earth surface reflectivity climatology at 340–380 nm from TOMS data, *J. Geophys. Res.*, *102*(D23), 28,003–28,011.

Jancic, Z. I. (1994), The step-mountain Eta coordinate model: Further developments of the convection, viscous sublayer and turbulence closure schemes, *Mon. Weather Rev.*, *122*, 927–945.

Kalnay, E., et al. (1996), The NCEP/NCAR 40-year reanalysis project, *Bull. Am. Meteorol. Soc.*, *77*, 437–471.

Kaufman, Y. J., I. Koren, L. A. Remer, D. Tanre, P. Ginoux, and S. Fan (2005), Dust transport and deposition observed from the TERRA-MODIS space observations, *J. Geophys. Res.*, *110*, D10S12, doi:10.1029/2003JD004436.

Kishcha, P., P. Alpert, J. Barkan, I. Kirchner, and B. Machenhauer (2003), Atmospheric response to Saharan dust deduced from ECMWF reanalysis (ERA) temperature increments, *Tellus, Ser. B*, *55*(4), 901–913.

Liou, K.-N. (1980), *An Introduction to Atmospheric Radiation*, Elsevier, New York.

Moulin, C., C. E. Lambert, F. Dulac, and U. Dayan (1997), Control of atmospheric export of dust from North Africa by the North Atlantic Oscillation, *Nature*, *387*, 691–694.

Nickovich, S., A. Papadopoulos, O. Kakaliagou, and G. Kallos (2001), Model for prediction of desert dust cycle in the atmosphere, *J. Geophys. Res.*, *106*, 18,113–18,130.

Prospero, J. M., P. O. Ginoux, S. Torres, E. Nicholson, and T. E. Gill (2002), Environmental characterization of global sources of atmospheric soil dust identified with the NIMBUS 7 Total Ozone Mapping Spectrometer (TOMS) absorbing aerosol product, *Rev. Geophys.*, *40*(1), 1002, doi:10.1029/2000RG000095.

Shao, Y., M. R. Raupach, and P. A. Findlater (1993), Effect of saltation bombardment on the entrainment of dust and wind, *J. Geophys. Res.*, *98*, 12,719–12,726.

Shay-El, Y., P. Alpert, and A. da Silva (1999), Reassessment of the moisture source over the Sahara Desert based on NASA reanalysis, *J. Geophys. Res.*, *104*, 2015–2030.

Stull, R. B. (1988), *Introduction to Boundary Layer Meteorology*, 666 pp., Springer, New York.

Torres, O., P. K. Bhartia, J. R. Herman, A. Sinyuk, P. Ginoux, and B. Holben (2002), A long-term record of aerosol optical depth from TOMS observations and comparison to AERONET measurements, *J. Atmos. Sci.*, *59*, 398–413.

Washington, R., M. Todd, N. J. Middleton, and A. S. Goudie (2000), Dust storm source areas determined by the Total Ozone Monitoring Spectrometer and surface observations, *Ann. Assoc. Am. Geogr.*, *93*(2), 297–313.

P. Alpert, J. Barkan, and P. Kishcha, Department of Geophysics and Planetary Sciences, Tel-Aviv University, Tel-Aviv 69978, Israel. (pinhas@cyclone.tau.ac.il)